

# Sustained NMDA Receptor Hypofunction Induces Compromised Neural Systems Integration and Schizophrenia-Like Alterations in Functional Brain Networks

Neil Dawson<sup>1,2,3</sup>, Xiaolin Xiao<sup>4,5</sup>, Martin McDonald<sup>2,6</sup>, Desmond J. Higham<sup>2,4</sup>, Brian J. Morris<sup>1,7</sup> and Judith A. Pratt<sup>1,2,3</sup>

<sup>1</sup>Psychiatric Research Institute of Neuroscience in Glasgow (PsyRING), Glasgow, UK, <sup>2</sup>Centre for Neuroscience, University of Strathclyde (CeNsUS), Glasgow, UK, <sup>3</sup>Strathclyde Institute of Pharmacy and Biomedical Sciences (SIPBS), University of Strathclyde, 161 Cathedral Street, Glasgow, G4 0RE, UK, <sup>4</sup>Department of Mathematics and Statistics, University of Strathclyde, 26 Richmond Street, Glasgow, G1 1XH, UK, <sup>5</sup>Integrative Genomics and Medicine Group, MRC Clinical Sciences Centre, Imperial College London, Du Cane Road, London, W12 0NN, UK, <sup>6</sup>Department of Bioengineering, University of Strathclyde, 106 Rottenrow East, Glasgow, G4 0NW, UK, <sup>7</sup>Institute of Neuroscience and Psychology, College of Medical, Veterinary and Life Sciences, University of Glasgow, West Medical Building, G12 8QQ, UK

Address correspondence to Neil Dawson, Strathclyde Institute of Pharmacy and Biomedical Sciences (SIPBS), University of Strathclyde, 161 Cathedral Street, Glasgow, G4 0RE, UK. Email: neil.dawson@strath.ac.uk

**Compromised functional integration between cerebral subsystems and dysfunctional brain network organization may underlie the neurocognitive deficits seen in psychiatric disorders. Applying topological measures from network science to brain imaging data allows the quantification of complex brain network connectivity. While this approach has recently been used to further elucidate the nature of brain dysfunction in schizophrenia, the value of applying this approach in preclinical models of psychiatric disease has not been recognized. For the first time, we apply both established and recently derived algorithms from network science (graph theory) to functional brain imaging data from rats treated subchronically with the N-methyl-D-aspartic acid (NMDA) receptor antagonist phencyclidine (PCP). We show that subchronic PCP treatment induces alterations in the global properties of functional brain networks akin to those reported in schizophrenia. Furthermore, we show that subchronic PCP treatment induces compromised functional integration between distributed neural systems, including between the prefrontal cortex and hippocampus, that have established roles in cognition through, in part, the promotion of thalamic dysconnectivity. We also show that subchronic PCP treatment promotes the functional disintegration of discrete cerebral subsystems and also alters the connectivity of neurotransmitter systems strongly implicated in schizophrenia. Therefore, we propose that sustained NMDA receptor hypofunction contributes to the pathophysiology of dysfunctional brain network organization in schizophrenia.**

**Keywords:** 2-deoxyglucose autoradiographic imaging, graph theory, network science, phencyclidine

## Introduction

Schizophrenia is a chronic psychiatric disorder characterized by positive symptoms (e.g. hallucinations), negative symptoms (e.g. avolition), and cognitive deficits. The cognitive deficits in this disorder are evident in multiple domains including executive functioning (e.g. behavioral flexibility) and memory. Complex cognitive tasks, such as those requiring behavior flexibility, are comprised of multiple discrete cognitive components, such as working memory and attention, that localize to discrete neural subsystems within the brain. Functional integration between these distributed subsystems is essential for effective cognitive functioning. Compromised functional integration between neural subsystems is hypothesized to underlie the cognitive deficits seen in

schizophrenia (Peled et al. 2001; Kim et al. 2003; Honey et al. 2005). Indeed, functional imaging studies suggest that compromised integration between the prefrontal cortex (PFC) and hippocampus (HP; Meyer-Lindenberg et al. 2005; Benetti et al. 2009) and between cortical regions (Friston and Frith 1995; Kim et al. 2005) underlie the cognitive deficits in schizophrenia. However, insight gained from these studies may be limited by the a priori selection of the functional interactions of interest, plausibly over-emphasizing the importance of a given interaction and missing others that are biologically relevant. Taking a systems biology approach to modeling functional brain networks offers a new opportunity to identify compromises in functional integration that may be missed with a reductionist approach. Indeed, considering altered brain connectivity in the context of complex brain networks, from a network science perspective, has recently provided added insight into the nature of disturbed brain functioning in schizophrenia (Micheloyannis et al. 2006; Bassett et al. 2008; Liu et al. 2008).

There is a compelling evidence to support a role for prolonged N-methyl-D-aspartic acid (NMDA) receptor hypofunction in schizophrenia. NMDA receptor antagonists are widely used in clinical and preclinical research to probe altered glutamatergic transmission in the disorder. While acute treatment with NMDA receptor antagonists, such as ketamine, appears to recapitulate the acute psychotic symptoms and depersonalized states of the disorder, chronic NMDA antagonists treatment regimes appear to be more closely related to the chronic deficit syndrome (cognitive deficits and negative symptoms) of the disorder. For example, humans who chronically use the NMDA receptor antagonist phencyclidine (PCP) display cognitive deficits (Cosgrove and Newell 1991) and reduced PFC activity (“hypofrontality”, Hertzmann et al. 1990; Wu et al. 1991) characteristic of chronic schizophrenia. Importantly, the cognitive deficits and disease-relevant pathology induced by chronic NMDA receptor treatment regimes endure for considerable periods of time after the cessation of treatment (Egerton et al. 2005, 2008; Dawson et al. 2012; Pratt et al. 2012).

The translational animal model of repeated subchronic PCP exposure, which induces sustained NMDA receptor hypoactivity, effectively reproduces the cognitive deficits seen in schizophrenia (Egerton et al. 2005, 2008; Dawson et al. 2012). Furthermore, subchronic PCP treatment produces overt alterations in cerebral metabolism (e.g. hypofrontality),

reduces expression of the gamma-aminobutyric acidergic marker parvalbumin, and induces alterations in neurochemistry and receptor expression that parallel those seen in this disorder (Cochran et al. 2002, 2003; Steward et al. 2004; Pratt et al. 2008). Moreover, we have recently confirmed that the pharmacological basis of the cognitive and functional deficits seen in this translational model directly parallels that in schizophrenia (Dawson et al. 2012). However, the potential relationship between NMDA receptor hypofunction and compromised functional integration within the brain, or altered functional brain network structure, is yet to be established.

2-Deoxyglucose (2-DG) autoradiographic imaging (Sokoloff et al. 1977) allows the quantification of cerebral glucose utilization, as a reflection of functional activity, in animal models. Until recently (Dawson et al. 2011, 2012), the analysis of 2-DG data was confined to the direct statistical comparison of overt alterations in metabolism in discrete brain regions, and alterations at a systems level have not been investigated. Topological measures based on the algorithms of network science provide us with the opportunity to quantify the alterations in functional brain connectivity from 2-DG data on a global, subsystem and regional scale. Given that recent studies have begun to quantify brain network alterations in schizophrenia through the application of these algorithms, it is particularly timely to apply them in a preclinical setting. Here, we test the hypothesis that sustained NMDA receptor hypofunction contributes to the alterations in brain network structure seen in schizophrenia. We also identify the alterations in brain network structure in this translational model that provide new, quantitative, insight into disrupted brain functioning in schizophrenia.

## Materials and Methods

All experiments were completed using male Lister Hooded rats (Harlan-Olac, United Kingdom) housed under standard conditions (21 °C, 45–65% humidity, 12-h dark/light cycle [lights on 0600 h]). All experimental manipulations were carried out at least 1 week after entry into the facility, and all experiments were carried out under the Animals (Scientific Procedures) Act 1986. Animals received either sub-chronic treatment with vehicle (0.9% saline, intraperitoneally [i.p.],  $n=7$ ) or 2.58 mg kg<sup>-1</sup> PCP-HCl (i.p.,  $n=9$ , Sigma Aldrich, United Kingdom) once daily for 5 consecutive days (between 900 and 1100 h). The sub-chronic PCP treatment dosing regime utilized in this study has been shown to induce cognitive, behavioral, and neurochemical alterations, along with deficits in cerebral function, that have translational relevance to schizophrenia (Cochran et al. 2003; Steward et al. 2004; Egerton et al. 2005, 2008; Dawson et al. 2012). Furthermore, this dose of PCP is below the ED<sub>50</sub> for PCP-induced cell death (Olney et al. 1989), which could confound the translational relevance of this model to schizophrenia. In addition to PCP-treated animals, a group of animals received either acute treatment with modafinil (64 mg kg<sup>-1</sup> in 0.5% methylcellulose, per os [o.p.],  $n=6$ ) or vehicle (0.5% methylcellulose, o.p.,  $n=7$ ) to test the hypothesis that PCP-induced alterations in network organization were specifically induced by NMDA receptor hypofunction.

### Semiquantitative [<sup>14</sup>C]-2-DG Autoradiographic Imaging

Local cerebral glucose utilization (LCGU) was determined 72 h after the last administration of the sub-chronic treatment (saline, PCP) in accordance with previously published protocols (Dawson et al. 2011, 2012). This ensures that any pretreatment effects observed are independent of the acute effects of PCP administration. The semiquantitative 2-DG protocol used here determines the rate of metabolism in each brain region over the 45-min period following tracer injection.

Rats were injected i.p. with 4.625 MBq/kg of [<sup>14</sup>C]-2-DG (Perkin-Elmer, United Kingdom) at a steady rate over a 10-s period before being returned to their home cage. At exactly 45 min after isotope injection, animals were decapitated and a terminal blood sample was collected by torso inversion in heparinized weigh boats. The brain was rapidly dissected out intact then frozen in isopentane (−40 °C) and stored at −80 °C until sectioning. Blood samples were centrifuged to separate the plasma, and aliquots were removed for the determination of plasma glucose (10 μL) and [<sup>14</sup>C] (20 μL) concentrations by the semiautomated glucose oxidase assay (Beckman Glucose Analyser) and liquid scintillation analysis (Packard), respectively.

Frozen brains were sectioned (20 μm) in the coronal plane in a cryostat (−20 °C). A series of 3 consecutive sections were retained from every 200 μm, thaw mounted, and rapidly dried on a hot plate (70 °C). Autoradiograms were generated by apposing these sections, together with precalibrated [<sup>14</sup>C] standards (40–1069 nCi/g tissue equivalents: Amersham International, United Kingdom) to X-ray film (Kodak, SB-5) for 5 days. Autoradiographic images were analyzed by a computer-based image analysis system (MCID/M5+). The local isotope concentration for each brain region of interest (RoI) was derived from the optical density of autoradiographic images relative to that of the coexposed [<sup>14</sup>C] standards. Measurements were taken from 64 anatomically distinct brain regions defined with reference to a stereotactic rat brain atlas (Paxinos and Watson 1998). The rate of metabolism, LCGU, in each RoI, was determined as the ratio of [<sup>14</sup>C] present in that region relative to the average [<sup>14</sup>C] concentration in the whole brain of the same animal, referred to as the [<sup>14</sup>C]-2-DG uptake ratio. Whole-brain average [<sup>14</sup>C] levels were determined from the average [<sup>14</sup>C] concentration across all sections in which a RoI was measured. The significance of overt alterations in cerebral metabolism between experimental groups was tested using Student's *t*-test (2-tailed) with a significance set at  $P < 0.05$ .

### Inter-Regional Correlations and Functional Brain Networks

The inter-regional Pearson's correlation coefficient (partial correlation) was used as the metric of the functional association between brain regions, generated from the [<sup>14</sup>C]-2-DG uptake ratios for each region, across all animals within the same experimental group (i.e. either control or PCP treated). These correlations were Fisher transformed to give the correlation data a normal distribution. This resulted in a pair of 64 × 64 partial correlation matrices, each within-group matrix representing the specific association strength between each of the 2016 possible pairs of regions. From each partial correlation matrix ( $R$ ), we derived a binary adjacency matrix ( $A$ ) where the functional connection between 2 regions ( $a_{i,j}$  element) was zero if the Pearson's correlation coefficient was lower than the defined threshold ( $P_{|i,j|} < T$ ) and unity if the coefficient was greater or equal to the defined threshold ( $P_{|i,j|} > T$ ). The adjacency matrix can also be represented as an undirected graph  $G$ , where a line or edge represents the functional interaction between 2 brain regions (nodes) if the partial correlation coefficient exceeds the defined threshold value.

### Network Analysis

Bullmore and Sporns (2009) have recently highlighted the added insight that may be gained from applying the algorithms of network science to the complex brain imaging data gained in a clinical context. Here, we consider functional brain network architecture at the global, divisional, and regional scales in brain imaging data gained in a preclinical context. Global network architecture was quantified in terms of the mean degree ( $\langle k \rangle$ ), average path length ( $L_p$ ), and mean clustering coefficient ( $C_p$ ) of the whole-brain network. These measures quantitatively define global brain network connectivity, efficiency, and clustering, respectively (outlined in greater detail in the section on Global Network Architecture). Regional properties were defined in terms of degree ( $k$ ), betweenness ( $B_c$ ), and closeness ( $C_c$ ) centrality. These measures allow us to quantitatively define which brain regions are hubs in each of the brain networks, and how regional hub status is altered by PCP treatment (outlined in

greater detail in the section on Regional Centrality and Hub Region Identification).

Alterations in divisional architecture were determined in terms of altered functional clustering, identified in the brain networks through the application of a recently proposed generalized singular value decomposition (GSVD) algorithm (Xiao et al. 2011), that provides a data-driven approach to identifying clustering difference between 2 matrices. This algorithm allows us to quantitatively determine how brain regions are functionally clustered exclusively in the brain network of one experimental group but not the other (outlined in greater detail in the section on Divisional Architecture). Global and regional metrics were determined on the binary adjacency matrices generated over a range of correlation thresholds (Pearson's  $r=0.3-0.4$  at 0.01 intervals, Fisher's  $z=0.309-0.424$ ). The upper limit of this threshold range was used to ensure that the resulting networks were fully connected, with none of the 64 brain regions (nodes) becoming functionally disconnected from the main body of the network. This allows for the direct and valid statistical comparison of the properties of the functional brain networks between the experimental groups. Regional metrics were determined by comparing the centrality measures in the real networks with that in calibrated (Erdős-Rényi) random graphs (1000 random graphs at each correlation threshold, 11 000 random graphs in total). The network analysis algorithms applied in our study, and the statistical approaches used in the analysis of these data, have previously been utilized in the analysis of brain imaging data gained in a clinical context (Micheloyannis et al. 2006; Bassett et al. 2008; Liu et al. 2008; Lynall et al. 2010), with the exception of the GSVD algorithm, which has been validated through its application to synthetic and metabolomics data sets (Xiao et al. 2011).

#### Global Network Architecture

Here, we provide brief, formal definitions of the global network metrics determined in this study, including mean degree ( $\langle k \rangle$ ), average path length ( $L_p$ ), and mean clustering coefficient ( $C_p$ ). The degree of a node ( $k$ ) is simply the number of edges that connect that node to the network, so highly connected nodes have a high degree. The mean degree ( $\langle K \rangle$ ) is the average number of edges of all the nodes in the network. A sparse network therefore has a low mean degree:

$$\langle K \rangle = \frac{1}{N} \sum_{i \in G} k_i. \quad (1)$$

The minimum path length between 2 nodes in a graph ( $L_{ij}$ ) is the smallest number of edges that must be traversed to make a connection between them. If 2 nodes are immediate neighbors, directly connected by a single edge, then  $L_{ij} = 1$ . The average path length ( $L_p$ ), or average  $L_{ij}$  across all possible pairs, is the average number of steps along the shortest paths for all nodes in the network. This provides a measure of global network efficiency, where networks with a low average path length are more efficient:

$$L_p = \frac{1}{2N(N-1)} \sum_{i>j} L_{ij}. \quad (2)$$

The clustering coefficient ( $C$ ) for a given node is the fraction of pairs of neighbors that are themselves connected. It provides an indication of how well connected the neighborhood of a node is. The mean clustering coefficient ( $C_p$ ) is the average clustering coefficient of all of the nodes in the network, which provides a measure of the local density or cliquishness of the network. A high mean clustering coefficient suggests high clustering and so efficient local information transfer:

$$C_p = \frac{1}{N} \sum_{i \in G} C_i. \quad (3)$$

The significance of PCP-induced alterations in the global properties of 2-DG functional brain networks was determined by the comparison of the real difference in each measure with that of networks generated from 5000 random permutations of the raw 2-DG data at each correlation threshold (55 000 random permutations in total). The

significance was set at  $P < 0.05$  and was determined from the average  $P$ -value across the entire correlation threshold range analyzed.

#### Regional Centrality and Hub Region Identification

In this study, we consider node centrality as determined by degree ( $k_i$ ), betweenness ( $B_c$ ), and closeness ( $C_c$ ). Degree centrality is based on the number of nodal connections. Betweenness centrality ( $B_c$ ) is based on the fraction of shortest paths that go through a given node,  $i$ :

$$B_c(i) = \sum_{\substack{s \neq i \neq t \in G \\ s \neq t}} \frac{\sigma_{st}(i)}{\sigma_{st}}. \quad (4)$$

Here,  $\sigma_{st}$  denotes the total number of shortest paths from  $s$  to  $t$  and  $\sigma_{st}(i)$  denotes the number of shortest paths from  $s$  to  $t$  that go through a node ( $i$ ). Closeness centrality ( $C_c$ ) is based on the mean geodesic distance of a node to all other reachable nodes in the network:

$$C_c(i) = \frac{1}{\sum_{t \in G \setminus i} d_G(i, t)}. \quad (5)$$

A brain region may be considered to be an important hub region in the network if it has a high degree, betweenness or closeness centrality. In this study, a brain region was defined as a hub, in the 2-DG functional brain network of either control (vehicle-treated) or PCP-treated animals, if, for any centrality measure, the regional centrality measure in the real network relative to that of calibrated random Erdős-Rényi graphs (1000 random graphs at each correlation threshold, 11 000 random graphs in total), was  $z > 1.96$ . The  $z$ -score for each centrality measure was calculated as shown below. The formula below outlines the  $z$ -score calculation for betweenness centrality ( $B_c$ ) of node  $i$  for illustrative purposes:

$$Z\text{-score } B_c(i) = \frac{B_c^{\text{real}} - B_c^{\text{random}}}{\text{Standard Deviation}_{(B_c^{\text{random}})}}. \quad (6)$$

The significance of PCP-induced alterations in regional centrality was determined by the comparison of the  $z$ -score difference in regional centrality in the real brain networks relative to that in networks generated from 11 000 random permutations of the raw 2-DG data (1000 random permutations at each correlation threshold). The significance was set at  $P < 0.05$ .

#### Divisional Architecture

Differences in the divisional architecture of the functional brain networks between experimental groups were characterized through the application of a recently developed algorithm for cluster identification based on the GSVD (Xiao et al. 2011). In the context of this study, the aim of applying this algorithm to the data was to identify functional clusters of brain regions exclusive to only one of the experimental groups. In essence, this algorithm allows the reordering of 2 square, symmetric, real-value matrices  $A$  and  $B$  with the aim of discovering a new node (brain region) ordering, by assigning each node to a new coordinate ( $z_i$ ) on a one-dimensional axis, that reveals clusters of nodes that exhibit strong functional connectivity (mutual weights) exclusive to one network. In its original application (Xiao et al. 2011), the algorithm was justified mathematically through the variational properties of the GSVD and was demonstrated to give biologically meaningful results. Here, we give a new interpretation of the algorithm that we believe will help to clarify its role to non-experts. We do this by exploiting the fact that the GSVD can be computed for an iteration. In this way, we can regard the position of each brain region ( $i$ ) in the final ordering as arising from a shuffling process that takes the form

$$z_i^{[k+1]} = \frac{\hat{a}_{ii}}{\hat{b}_{ii}} \left( z_i^{[k]} + \sum_{l=1, l \neq i}^N \frac{\hat{a}_{il}}{\hat{a}_{ii}} z_l^{[k]} \right) - \sum_{l=1, l \neq i}^N \frac{\hat{b}_{il}}{\hat{b}_{ii}} z_l^{[k+1]}, \quad (7)$$

where each brain region is shuffled iteratively from its arbitrary position in the original ordering,  $\{z_i^{[0]}\}_{i=1}^N$ , using the information contained in the 2 matrices, until a stable reordering emerges. The relevant information used for the iterative reordering of the matrices are the generalized degrees

$$\hat{a}_{ii} = \sum_{j=1}^N a_{ij}^2 \quad \text{and} \quad \hat{b}_{ii} = \sum_{j=1}^N b_{ij}^2 \quad (8)$$

that measure the overall strength of a region,  $i$ , in each network and the pairwise measures

$$\hat{a}_{il} = \sum_{j=1, j \neq i}^N a_{ij} a_{jl} \quad \text{and} \quad \hat{b}_{il} = \sum_{j=1, j \neq i}^N b_{ij} b_{jl} \quad (9)$$

that quantify the connectivity between 2 regions,  $i$  and  $l$ , in each network. This value is large if the 2 regions,  $i$  and  $l$ , have many strong connections to common neighbors.

In the overall iteration (7), if we suppose that a collection of regions have been given large positive coefficients, because they represent a cluster exclusive to that experimental network, the region  $i$  will be moved toward this group and considered to be part of this cluster if

1.  $a_{ij}/b_{ii}$  is large, so that region  $i$  is relatively important in network  $A$  and
2.  $a_{il}/a_{ii}$  is large for regions in this current cluster, so that region  $i$  is relatively well connected with this group in network  $A$ .

In contrast, because of the minus sign in (equation 7), region  $i$  will move away from this current cluster if

3.  $b_{il}/b_{ii}$  is large for regions in this current cluster, so that region  $i$  is relatively well connected with this group in network  $B$ .

So overall, region  $i$  will be moved toward this current cluster, in the sense that its new coefficient  $z_i^{[k+1]}$  will be made larger than its previous coefficient  $z_i^{[k]}$ , if it is strongly connected to these regions in  $A$ , but not strongly connected in  $B$ . As the iteration proceeds, that is, as  $k$  increases, the brain regions settle into a final stable reordering, equivalent to that used in Xiao et al. (2011). In this final reordering, brain regions that are strongly functionally connected, forming a functional cluster, in group  $A$  but not in group  $B$ , are assigned nearby positions at either end of the one-dimensional axis (reordering). Of course, by reversing their roles in (equation 7), we may also compute an ordering that emphasizes clusters present in the group  $B$  that are not present in the group  $A$ .

In the case of our data, matrices  $A$  and  $B$  are comprised of the real-value inter-regional correlation coefficients (Pearson's coefficient Fisher  $z$ -transformed) for the control and PCP treatment groups, respectively. These matrices are identical to those used for the generation of the binary adjacency matrices to characterize the global and regional characteristics of the functional brain networks in these experimental groups. Once the matrices have been reordered through this iterative algorithm, the significant presence of a cluster in the given network was tested by the comparison of a cluster quality measure  $[c(A,B)]$

$$\frac{\text{density of edges within the cluster in } B / \text{density of edges outside the cluster in } B}{\text{density of edges within the cluster in } A / \text{density of edges outside the cluster in } A} \quad (10)$$

for a defined node set, giving a good cluster in one of the networks ( $B$ ) but not the other ( $A$ ), relative to that in 1000 random permutations of the initial matrices, as previously outlined (Xiao et al. 2011).

#### Hypergeometric Probability Testing

The hypergeometric probability test was used to calculate the probability of finding at least the observed number brain regions from a given neural subsystem in the clusters identified through the GSVD

algorithm. These neural subsystems were based on localized subfields either with known high interconnectivity (e.g. subfields of the HP) or with well-defined connectivity (e.g. basal ganglia). The hypergeometric probability test was used to identify whether any of the 10 defined subsystems were significantly over-represented in any of the GSVD identified clusters. In addition to these 10 defined subsystems, the probability of observing an over-representation of the hub brain regions, as identified through centrality analysis in this study, in any of the GSVD-defined clusters was also investigated.

In its general form, exact hypergeometric probability allows the calculation of the probability of observing at least  $x$  brain regions from a prespecified cluster of  $m$  brain regions when  $n$  regions are chosen at random from a total of  $N$ . The probability is calculated as:

$$\sum_{k=x}^m \frac{\binom{m}{k} \binom{N-m}{n-k}}{\binom{N}{n}},$$

where parentheses denote the binomial coefficient:

$$\binom{a}{b} = \frac{a!}{b!(a-b)!}.$$

The significant over-representation of a given functional group in any GSVD-defined significant cluster was set at a hypergeometric probability of  $P < 0.005$ , as a Bonferroni-type correction was applied to the probability value to account for the effect of multiple comparison in investigating 10 defined functional groups ( $P < 0.05/10$ ).

The effect of acute modafinil treatment on overt alterations in cerebral metabolism and divisional architecture, using the same analytical framework as applied to the subchronic PCP data set (GSVD analysis followed by hypergeometric probability testing), was used in order to confirm the specificity of subchronic NMDA receptor hypofunction in promoting the pattern of neural system disintegration seen in PCP-treated animals. The data for this group are shown in the Supplementary Material, Section 2. Acute modafinil challenge was chosen as an appropriate positive pharmacological control as while modafinil treatment enhances dopaminergic, noradrenergic, and serotonergic neurotransmission (Ferraro et al. 2000; Hilaire et al. 2001; Madras et al. 2006; Minzenberg and Carter 2008), the drug has negligible affinity for NMDA receptors (Mignot et al. 1994). Furthermore, acute modafinil treatment does not induce deficits in the same cognitive domains as those seen in animals treated subchronically with PCP (Waters et al. 2005). In fact, acute modafinil treatment has been shown to reverse translationally relevant deficits in these distinct cognitive domains in preclinical models relevant to schizophrenia (Redrobe et al. 2010; Dawson et al. 2012) and also schizophrenia patients (Turner et al. 2004), but has a limited effect in these cognitive domains in health controls (Randall et al. 2003).

## Results

### PCP-Induced Alterations in Overt Cerebral Metabolism

The subchronic PCP treatment produced significant, regionally selective, alterations in the overt rate of cerebral metabolism in 9 of the 64 brain regions analyzed (Table 1), as determined using the semiquantitative 2-DG autoradiographic imaging technique (Dawson et al. 2011, 2012). In particular, subchronic PCP treatment induced hypofrontality, a reduced rate of metabolism in PFC regions, including in the anterior prefrontal cortex (PrL) and orbital (lateral and dorsolateral) cortex, and a reduced rate of metabolism in discrete thalamic nuclei (dorsal reticular [dRT] and centromedial [CMthal] thalamus and the nucleus reuniens [Re]). In addition to PFC regions, PCP treatment induced hypometabolism in the retrosplenial cortex, part of the cingulate cortex and in the

**Table 1**  
PCP-induced alterations in overt cerebral metabolism

Region	Control Mean $\pm$ SEM	PCP Mean $\pm$ SEM
Anterior PrL	1.266 $\pm$ 0.031	1.154* $\pm$ 0.034
LO cortex	1.753 $\pm$ 0.033	1.555** $\pm$ 0.043
DLO cortex	1.153 $\pm$ 0.027	1.074* $\pm$ 0.030
RSC	1.526 $\pm$ 0.030	1.426** $\pm$ 0.016
dRT	1.330 $\pm$ 0.024	1.232* $\pm$ 0.033
CMthal	1.134 $\pm$ 0.047	1.010* $\pm$ 0.029
Re	1.277 $\pm$ 0.043	1.134* $\pm$ 0.044
DLST	1.257 $\pm$ 0.025	1.181* $\pm$ 0.021
BST	0.590 $\pm$ 0.015	0.663** $\pm$ 0.013

Subchronic PCP treatment induces localized, significant alterations in cerebral metabolism. PCP induces significant hypometabolism in the anterior prelimbic (PrL), lateral (LO) and dorsolateral (DLO) orbital cortices, the retrosplenial cortex (RSC), dorsal reticular thalamus (dRT), centromedial thalamus (CMthal), nucleus reuniens (Re), and dorsolateral striatum (DLST). Subchronic PCP induced significant hypermetabolism in the bed nucleus of the stria terminalis (BNST). Data shown as the mean  $\pm$  SEM 2-DG uptake ratio.

\* $P < 0.05$  and \*\* $P < 0.01$  significant difference in PCP-treated ( $n = 9$ ) when compared with control (vehicle-treated,  $n = 7$ ) animals (Student's  $t$ -test, 2-tailed).

dorsolateral striatum (DLST). In only 1 region, the bed nucleus of the stria terminalis, was metabolism significantly increased following subchronic PCP treatment. PCP-induced alterations in overt cerebral metabolism were highly localized and metabolism in the majority of the regions investigated remained unaltered, including in all subfields of the HP, the amygdala nuclei, and the septal nuclei. The PCP-induced alterations in overt cerebral metabolism in the PFC and reticular thalamus found in this study are consistent with those reported when using the quantitative 2-DG autoradiographic technique to characterize cerebral metabolism in animals treated with the same PCP treatment regime (Cochran et al. 2002; Dawson et al. 2012).

### PCP-Induced Alterations in Global Functional Brain Network Topology

Subchronic PCP treatment resulted in a functional brain network with reduced connectivity as evidenced by a significant reduction in the mean degree  $\langle k \rangle$ , the average number of functional connections each brain region has within the network, across the entire analyzed correlation threshold range (Fig. 1A). The functional brain network in PCP-treated animals also displays a significantly increased average path length ( $L_p$ ) in comparison with control animals (Fig. 1B). This means that the length of the shortest paths that must be traversed to reach 1 brain region from another, averaged across the entire network, is significantly increased in the brain network of PCP-treated animals (across the entire correlation threshold range analyzed). A low average path length is representative of efficient information transfer across the entire network, at a global level, suggesting that the efficiency of information transfer between brain regions is reduced in the brain network of PCP-treated animals. In addition to these alterations, the mean clustering coefficient ( $C_p$ ), a measure of local connectivity or cliquishness within a network, is significantly decreased in the functional brain network of PCP-treated animals, across all correlation thresholds (Fig. 1C). This suggests that the efficiency of local information transfer, between neighboring brain regions (nodes), is reduced in the functional brain network of PCP-treated animals, when network clustering is considered at the global level.

When the brain networks are considered at the same cost, in essence comparing the global properties of the networks when they have the same number of connections by allowing weaker functional correlations to be considered as connected in the brain network of PCP-treated animals, there is no significant difference in the average path length ( $L_p$ ) or mean clustering coefficient ( $C_p$ ) of the brain networks (Fig. 1D,E). This suggests that the reduced efficacy of functional coupling between brain regions, as indicated by a significantly reduced mean degree  $\langle k \rangle$  at any given correlation threshold, in PCP-treated animals underlies the reduced average path length ( $L_p$ ) and reduced mean clustering coefficient ( $C_p$ ) seen in the brain networks of these animals.

### PCP-Induced Alterations in Regional Functional Connectivity

In the functional brain network of control animals, 19 of the 64 brain regions analyzed were identified as important hubs (Fig. 2 and Table 2). Of the 19 hub regions identified in the control network, 7 were thalamic nuclei (dRT, ventral reticular thalamus [vRT], mediodorsal thalamus, ventrolateral thalamus [VLthal], centrolateral thalamus [CLthal], and CMthal) and 3 were hippocampal subfields (CA1, CA2, and CA3). The locus coeruleus (LC), the origin of noradrenergic innervation to the forebrain, was identified as having the greatest average centrality score in the functional brain network of control animals. Other hub regions identified included subfields of the medial PFC (mPFC; mPrL1 and mPrL2), amygdala nuclei (central [CeA] and basolateral [BLA]), and the lateral habenula.

There was a little overlap in the brain regions identified as important hubs in the control network when compared with those identified as hubs in the brain network of PCP-treated animals, with only the ventral pallidum being identified as an important hub in both brain networks. This suggests that the structural organization of the functional brain network was markedly altered by subchronic PCP treatment. Only 7 of the 64 regions analyzed were identified as hub regions in the brain network of PCP-treated animals. These included 2 regions of the PFC (PrL and M1), the subiculum of the HP (Sub), and the vertical limb of the diagonal band of Broca (VDB; Fig. 2 and Table 2).

A statistically significant reduction in regional centrality in the functional brain network of PCP-treated animals was found for 18 of the 64 brain regions analyzed (Table 3). This included significantly reduced centrality for 7 thalamic nuclei (anteromedial thalamus [AMthal], CLthal, CMthal, dRT, vRT, VLthal, and Re), the LC, and 3 amygdala nuclei (BLA, medial amygdala [MeA], and CeA). All of these regions, with the exception of the MeA, were previously identified as important hubs in the functional brain network of control animals. A statistically significant increase in regional centrality in PCP-treated animals was found for 6 regions, including the VDB, Sub, and substantia nigra pars compacta (SNC). All of these regions had previously been identified as important hubs in the functional brain network of PCP-treated animals.

### PCP-Induced Alterations in Functional Subsystem Clustering

In the section on Divisional Architecture we gave a new justification for the GSVD algorithm proposed and tested in Xiao et al. (2011) for determining differences in clustering between

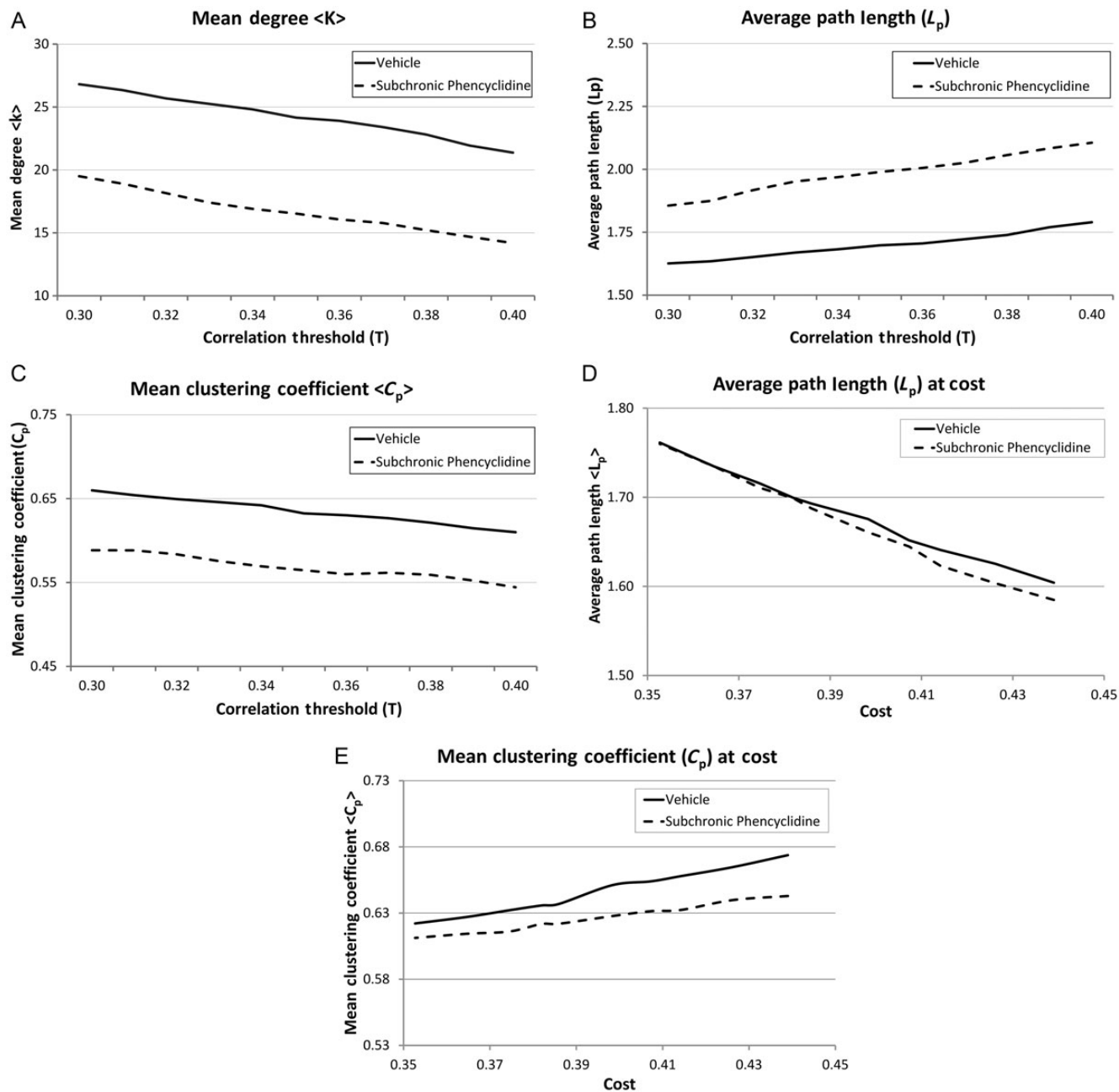


**Figure 1.** PCP-induced alterations in global functional brain network topography. Subchronic PCP treatment resulted in a functional 2-DG brain network with a significantly reduced (A) mean degree ( $P = 0.039$ ), increased (B) average path length ( $P < 0.001$ ), and reduced (C) clustering coefficient ( $P = 0.007$ ), when compared with that in control animals. When the functional brain networks of each experimental group were compared at the same cost, there was no significant difference between the two groups in terms of the (D) clustering coefficient ( $P = 0.097$ ) or (E) average path length ( $P = 0.175$ ). The significance of PCP-induced alterations in global network measures was analyzed in comparison with each measure in networks generated from 55 000 random permutations of the experimental data (5000 random permutations of the data at each 0.01 interval of the correlation threshold or cost range). The significance was set at  $P < 0.05$ .

2 networks based on the same set of nodes (brain regions). We used this approach to characterize PCP-induced alterations in the clustering arrangement of the functional brain networks. Subchronic PCP-induced alterations in regional clustering are suggestive of reduced functional integration between discrete neural subsystems (particularly between the HP, PFC, and the mPFC) through the loss of thalamic and hub brain region clusters. Through GSVD reordering, 3 significant (1 discrete and 2 overlapping) clusters of brain regions were identified as being present in control but not in PCP-treated

animals (Fig. 3). In PCP-treated animals, 3 significant clusters of brain regions were also identified that were not present in control animals. In control animals, hypergeometric probability revealed a significant over-abundance of basal ganglia structures in the discrete cluster [ $P(X \geq 4) = 4.19 \times 10^{-3}$ ] and a significant over-abundance of thalamic structures in both of the overlapping clusters [large cluster  $P(X \geq 11) = 1.74 \times 10^{-4}$ ; small cluster  $P(X \geq 6) = 1.92 \times 10^{-3}$ ; Table 4]. In addition, a significant over-abundance of control hub brain regions, previously identified in the brain network of control animals

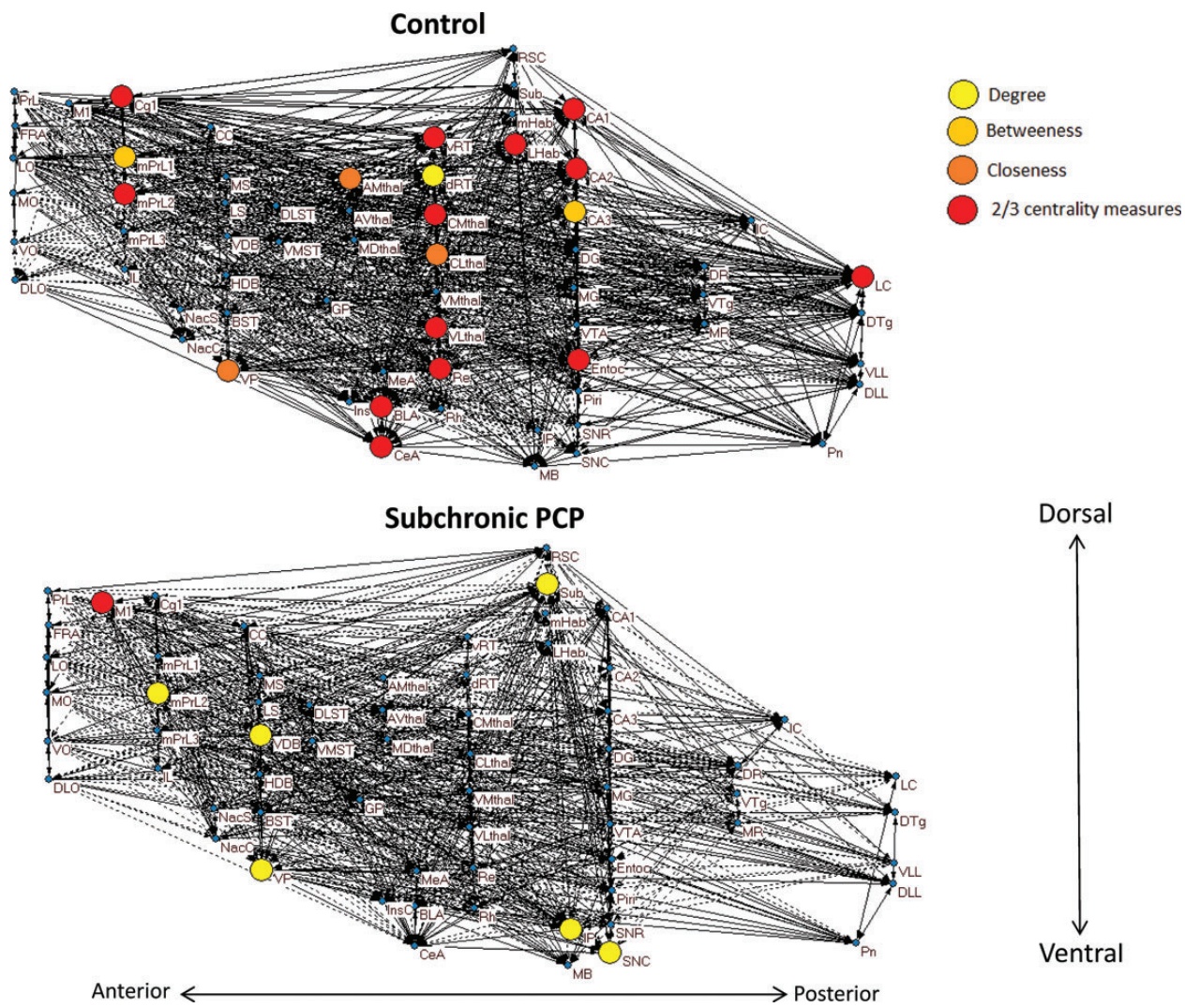


**Figure 2.** Hub brain regions in the functional brain network of control and PCP-treated rats. Graph representations of the functional 2-DG brain networks in (A) control and (B) PCP-treated animals. Brain networks are shown at the 0.4 correlation threshold ( $T = 0.4$ ). Brain regions (nodes) are placed in their approximate anterior to posterior and ventral to dorsal anatomical localization. Solid connections (edges) represent a positive correlation between cerebral metabolisms in 2 brain regions, whereas broken connections (edges) represent a negative correlation between cerebral metabolisms in 2 brain regions. If regional centrality, on any centrality measure, surpassed the  $z > 1.96$  threshold, calculated in comparison with 11 000 calibrated random Erdős-Rényi graphs, across the entire correlation threshold range ( $T = 0.3-0.4$ ) then that region was considered a hub in the functional brain network. Large nodes in the graph representations denote those regions considered to be hubs within the functional brain network. Node color denotes the centrality measure in which a brain region was considered to be an important hub in the network. These graphs were created using Pajek software (<http://pajek.imfm.si/doku.php?id=download>).

through centrality analysis, were found to be present in both of the overlapping clusters identified as being present in control but not in PCP-treated animals [large cluster  $P(X \geq 16) = 3.75 \times 10^{-4}$ , small cluster  $P(X \geq 9) = 1.29 \times 10^{-4}$ ]. These results suggest that the basal ganglia, thalamus, and the control hub brain regions are functionally clustered in control animals and that the functional connectivity of these neural subsystems is lost following subchronic PCP treatment. The finding that hub regions present in the control network are lost as a cluster in PCP-treated animals, as identified through this GSVD algorithm, is consistent with our finding that hub brain regions in control animals lose their centrality status in PCP-treated animals (Table 3) and that the functional brain network in control animals displays the property of assortativity (Fig. 4), where brain regions with a high degree of connectivity are connected to other brain regions of high connectivity.

In the functional brain network of PCP-treated animals, hypergeometric probability analysis revealed that one functional cluster present in PCP-treated but not in control animals has a significant over-abundance of PFC structures [ $P(X \geq 6) = 6.16 \times 10^{-6}$ ], another had a significant over-abundance of hippocampal structures [ $P(X \geq 5) = 3.31 \times 10^{-5}$ ], and the third cluster a significant over-abundance of the mPFC [ $P(X \geq 4) = 2.15 \times 10^{-3}$ ] subfields (Table 4). This suggests that in PCP-treated animals, these local, highly interconnected regions form discrete functional clusters that are not present under normal conditions (in control animals). In contrast to the effects of subchronic PCP treatment, acute treatment with modafinil failed to induce the functional segregation of PFC and hippocampal neural systems into distinct clusters, as determined by the application of GSVD analysis and hypergeometric probability testing (Supplementary Material, Section 2).

**Table 2**

Hub regions in the functional brain networks of control and PCP-treated animals

Region	Centrality measure			Average z-score
	Degree	Betweenness	Closeness	
<b>Hub regions in control animals</b>				
Locus coeruleus (LC)	<b>3.63</b>	0.80	<b>5.77</b>	3.40
Hippocampal CA2	<b>3.51</b>	0.68	<b>5.57</b>	3.25
Nucleus reuniens (Re)	<b>2.79</b>	<b>2.35</b>	<b>4.07</b>	3.07
Central amygdala (CeA)	<b>2.01</b>	<b>3.61</b>	<b>3.22</b>	2.95
Medial prefrontal cortex (layer 2, mPrL2)	<b>2.88</b>	1.84	<b>3.66</b>	2.79
Entorhinal cortex (EntoC)	<b>2.57</b>	1.58	<b>3.75</b>	2.63
Ventral reticular thalamus (vRT)	<b>3.23</b>	-0.20	<b>4.69</b>	2.57
Lateral habenula (LHab)	<b>2.46</b>	1.49	<b>3.48</b>	2.48
Basolateral amygdala (BLA)	<b>2.56</b>	0.28	<b>3.51</b>	2.12
Ventrolateral thalamus (VLthal)	<b>2.29</b>	1.28	<b>2.42</b>	2.00
Anteromedial thalamus (AMthal)	1.82	0.43	<b>2.66</b>	1.64
Hippocampal CA1	<b>2.06</b>	-0.51	<b>3.32</b>	1.62
Dorsal reticular thalamus (dRT)	<b>2.04</b>	0.81	1.89	1.58
Hippocampal CA3	0.64	<b>2.69</b>	0.97	1.42
Medial prefrontal cortex (layer 1, mPrL1)	1.49	-0.01	<b>2.42</b>	1.30
Cingulate cortex (Cg1)	<b>2.02</b>	-1.17	<b>2.44</b>	1.10
Ventral pallidum (VP)	1.37	-0.26	<b>2.10</b>	1.07
Centrolateral thalamus (CLthal)	1.37	-0.39	<b>2.05</b>	1.01
Centromedial thalamus (CMthal)	<b>2.01</b>	-1.12	<b>2.05</b>	0.98
<b>Hub regions in PCP-treated animals</b>				
Primary motor cortex (M1)	<b>2.46</b>	<b>3.67</b>	1.77	2.63
Medial prefrontal cortex (layer 2, mPrL2)	<b>3.06</b>	1.10	1.72	1.96
Hippocampal subiculum (Sub)	<b>3.58</b>	1.30	0.76	1.88
Ventral pallidum (VP)	<b>2.71</b>	0.26	0.79	1.25
Interpeduncular nucleus (IP)	<b>1.97</b>	1.12	0.52	1.20
Substantia nigra pars compacta (SNc)	<b>2.10</b>	0.54	0.40	1.01
Vertical limb of the diagonal band of Broca (VDB)	<b>1.96</b>	-0.29	0.29	0.65

Regions are listed in order of their ranked mean centrality z-score across all 3 centrality measures. The z-score for each centrality measure (degree, betweenness, and closeness), for each brain region (node), is also shown. Values in bold denote centrality measures in which a given brain region reaches the defined criteria [ $z\text{-score} > 1.96$  relative to 11 000 calibrated random Erdős-Rényi graphs across the entire correlation threshold range ( $T = 0.3\text{--}0.4$ )] to be considered as a hub brain region in the real experimental network.

## Discussion

Using a novel, quantitative, systems biology approach to modeling the functional preclinical brain imaging data gained using 2-DG imaging we have made important new insights into how sustained NMDA receptor hypoactivity impacts upon brain network structure. This has direct relevance for understanding the nature of brain dysfunction in schizophrenia. The alterations in global network structure found in the subchronic PCP translational model strongly parallel those reported in schizophrenia (Micheloyannis et al. 2006; Liu et al. 2008; Lynall et al. 2010). Furthermore, PCP-induced alterations in regional connectivity and in the functional clustering of neural subsystems support a role for NMDA receptor dysfunction in the compromised functional integration, particularly between the HP and PFC, reported in this disorder (Meyer-Lindenberg et al. 2005; Benetti et al. 2009). The compromised functional integration between these neural systems may be driven, in part, by reduced thalamus connectivity. These results provide strong experimental support for the hypothesis of NMDA receptor dysfunction in schizophrenia pathogenesis.

The reduced connectivity ( $k$ ), increased mean path length ( $L_p$ ), and reduced average clustering coefficient ( $C_p$ ) of the functional brain network in PCP-treated rats not only directly parallel the alterations reported in functional brain networks in schizophrenia (Micheloyannis et al. 2006; Liu et al. 2008; Lynall et al. 2010), but also suggest a functional brain network with a suboptimal organization that may contribute

**Table 3**

Hub brain regions showing altered centrality in PCP-treated animals

Region	Centrality measure			Average z-score difference
	Degree	Betweenness	Closeness	
<b>PCP-induced decreases in regional centrality</b>				
Locus coeruleus (LC)	<b>-6.23</b>	-1.16	<b>-11.79</b>	-6.39
Hippocampal CA2	<b>-4.71</b>	-2.50	<b>-9.57</b>	-5.59
Nucleus reuniens (Re)	<b>-4.10</b>	<b>-2.81</b>	<b>-6.54</b>	-4.49
Ventral reticular thalamus (vRT)	<b>-4.97</b>	1.22	<b>-8.07</b>	-3.94
Anteromedial thalamus (AMthal)	-4.24	-1.14	<b>-6.20</b>	-3.86
Medial amygdala (MeA)	-0.84	-3.43	<b>-5.64</b>	-3.30
Central amygdala (CeA)	-0.08	<b>-3.95</b>	<b>-4.90</b>	-2.98
Centromedial thalamus (CMthal)	<b>-2.77</b>	-0.48	<b>-4.86</b>	-2.70
Entorhinal cortex (EntoC)	<b>-1.28</b>	-1.98	<b>-4.48</b>	-2.58
Lateral habenula (LHab)	<b>-2.17</b>	-0.03	<b>-4.67</b>	-2.29
Basolateral amygdala (BLA)	<b>-1.55</b>	-0.55	<b>-4.69</b>	-2.27
Dorsal reticular thalamus (dRT)	<b>-3.30</b>	0.07	-3.03	-2.09
Medial prefrontal cortex (layer 1, mPrL1)	-0.74	-0.86	<b>-2.84</b>	-1.48
Centrolateral thalamus (CLthal)	-0.75	-0.54	<b>-2.94</b>	-1.41
Hippocampal CA1	<b>-0.58</b>	0.71	<b>-3.54</b>	-1.13
Ventrolateral thalamus (VLthal)	<b>-0.82</b>	-0.06	<b>-2.07</b>	-0.98
Medial prefrontal cortex (layer 2, mPrL2)	0.18	-0.73	<b>-1.94</b>	-0.83
Cingulate cortex (Cg1)	-0.27	0.94	<b>-2.46</b>	-0.60
<b>PCP-induced increases in regional centrality</b>				
Substantia nigra pars compacta (SNc)	<b>5.06</b>	2.65	6.32	4.68
Interpeduncular nucleus (IP)	<b>4.64</b>	3.50	4.39	4.18
Primary motor cortex (M1)	<b>1.58</b>	<b>5.29</b>	1.05	2.64
Vertical limb of the diagonal band of Broca (VDB)	<b>2.48</b>	1.77	1.43	1.89
<b>broca (VDB)</b>				
Hippocampal subiculum (Sub)	<b>2.35</b>	1.39	-0.95	0.93
Ventral pallidum (VP)	<b>1.34</b>	0.52	-1.32	0.18

Values shown are the difference in the z-score centrality measure of a given brain region in the PCP-treated network relative to the regional z-score centrality measure in the control network. Data are shown for degree, betweenness, and closeness centrality. Regions are ranked according to their mean loss or gain in centrality z-score across all centrality measures. Highlighted bold values are those where the z-score difference in regional centrality between the experimental groups is significantly ( $P < 0.05$ ) different from that of networks generated from 11 000 random permutations of the experimental data set, determined across the entire correlation threshold range ( $T = 0.3\text{--}0.4$ ).

to the cognitive deficits reported in these animals (Egerton et al. 2005, 2008; Dawson et al. 2012). A reduced mean degree ( $k$ ) and increased mean path length ( $L_p$ ) suggest that the efficiency of information transfer across the whole-brain network is impeded in PCP-treated animals. This suggests a suboptimal network organization where the efficiency of information transfer between distributed subsystems is impeded (compromised functional integration) following subchronic PCP treatment. The contention of compromised functional integration is further supported by the alterations in regional centrality and functional clustering seen in the brain networks of PCP-treated animals.

Alterations in regional centrality indicate that many network hubs, including multiple thalamic hub regions (dRT, vRT, AMthal, CMthal, CLthal, VLthal, and Re), lose their hub status in PCP-treated animals. Furthermore, the identification of thalamic regions as a functional cluster lost in the brain network of PCP-treated animals (Fig. 3), through the application of the GSVD algorithm, further reinforces the loss of thalamic connectivity in these animals. In addition, regions identified as hubs in the control brain network were also lost as a functional cluster in PCP-treated animals. The loss of both hub and thalamic region connectivities will contribute to the compromised functional integration seen in the brain networks of PCP-treated animals. The loss of thalamic region connectivity is particularly pertinent given the widespread anatomical connectivity of these regions and their established

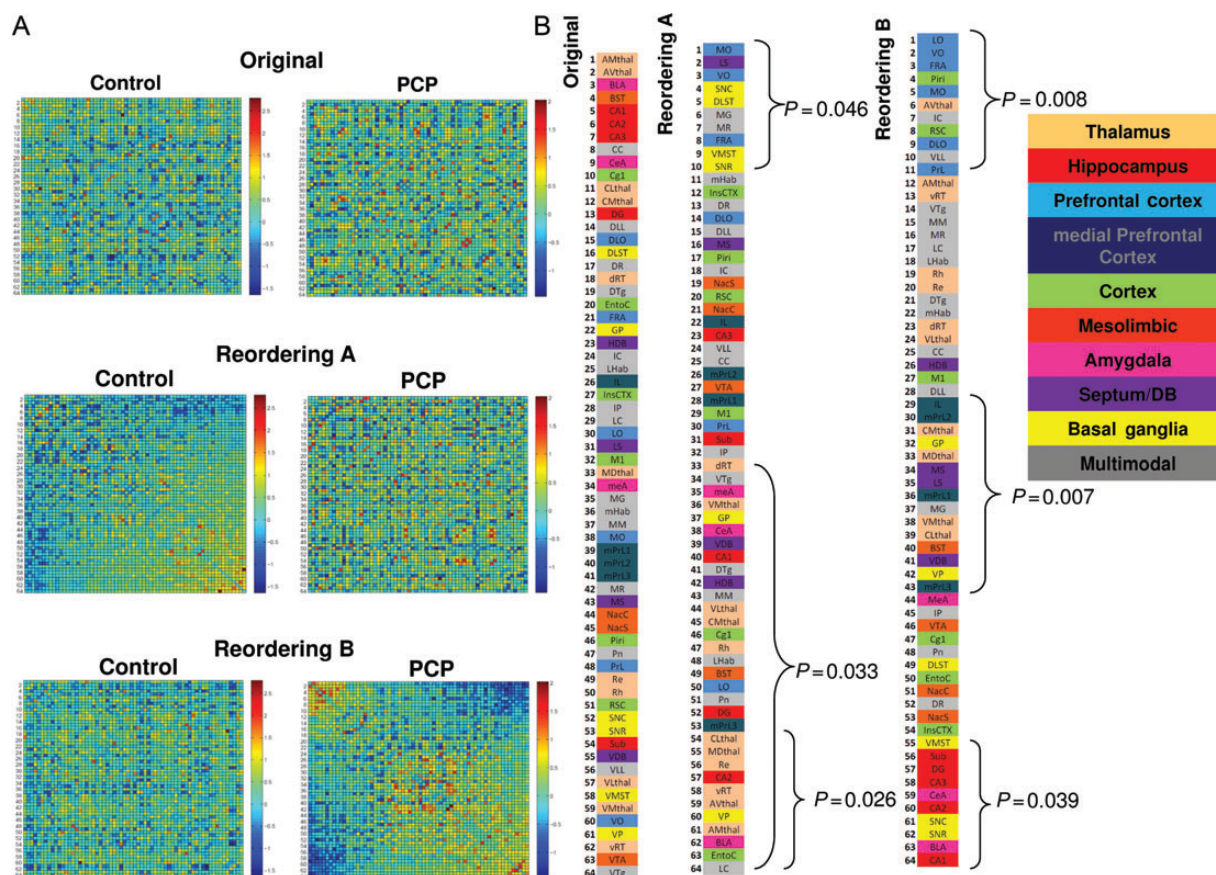


**Figure 3.** The functional clustering of brain regions is altered following subchronic PCP treatment. (A) Heatmaps showing the clustering of brain regions in control and PCP-treated animals in the original (alphabetically ordered) matrices and following GSVD reordering. Warm colors (red/orange) represent high/positive functional correlations between brain regions, and cold colors (blue/green) represent low/negative correlations between brain regions (Pearson's correlation coefficient Fisher transformed). Reordering A identifies brain region clusters present in the functional brain network of control animals that are not present in that of PCP-treated animals. Reordering B identifies brain region clusters present in the PCP-treated brain networks that are not present in the control network. Visually, there appear to be 1 cluster in control animals not present in PCP-treated animals and 3 clusters present in PCP-treated animals that are not present in control. (B) Brain region list showing the order of brain regions in the original and GSVD reordered matrices. In the brain list for reordering A, 3 significant clusters are present, which represent significant clusters in control animals that are not present in PCP-treated animals. In reordering B, 3 significant clusters were also identified that represent clusters in PCP-treated animals that are not present in the functional brain network of control animals. Significance ( $P < 0.05$ ) was established through the comparison of the cluster quality measure in the real networks relative to that in 1000 random permuted networks. When brain regions are color coded on the basis of established neural subsystems, these appear to display an over-abundance in some of the GSVD-defined clusters (e.g. hippocampal regions in the 55–64 significant cluster present in PCP but not in control animals, reordering B).

role as relay regions connecting to and regulating distributed functional brain subsystems (Guillery and Sherman 2002; Schmahmann and Pandya 2008). Moreover, the loss of thalamic functional connectivity is consistent with the impaired integrity of neurons within these regions in PCP-treated animals (Cochran et al. 2003), which directly parallel observations in schizophrenia (Danos et al. 1998). Furthermore, the impaired connectivity of thalamic regions in PCP-treated animals directly parallels the altered functional connectivity of these regions in schizophrenia (Andreasen et al. 1996; Welsh et al. 2010), a mechanism proposed to contribute to the compromised functional integration seen in this disorder (Friston and Frith 1995; Kim et al. 2005; Meyer-Lindenberg et al. 2005; Benetti et al. 2009) in accordance with the hypothesis of schizophrenia as a disconnection syndrome (Weinberger et al. 1992; Bullmore et al. 1997).

Compromised functional integration between distributed neural subsystems in the functional brain network of PCP-treated animals is also supported by the abnormal functional clustering of local, highly anatomically connected brain

regions in these animals (Fig. 3). Specifically, subfields of the HP, PFC, and mPFC become functionally segregated, discrete clusters of brain regions in PCP-treated animals, whereas in control animals, these regions are not discretely clustered. In particular, the segregation of HP and PFC regional clusters in PCP-treated animals suggests compromised functional integration between these subsystems, which directly parallels the altered functional coupling between these subsystems in schizophrenia (Meyer-Lindenberg et al. 2005; Benetti et al. 2009). When considered in the context of known anatomical connectivity, PCP-induced alterations in functional hub status provide evidence for disrupted functional connectivity in discrete anatomical pathways that may contribute to the compromised functional integration seen between the PFC and HP in these animals. In this way, disrupted functional integration between the PFC and HP in PCP-treated animals is mediated by disrupted connectivity of the indirect PFC–Re–HP pathway and in the direct HP–PFC projection. PFC regions receive direct, excitatory input from the HP (Ferino et al. 1987; Jay et al. 1995; Laroche et al. 2000). It has recently been shown

**Table 4**

Assignment of neural subsystems to the discrete functional clusters present in control or PCP-treated animals

Reordering	Cluster	P-value	Cluster size (n)	Functional group	Regions in subsystem (m)	Regions in cluster (x)	Hypergeometric probability $P(X \geq x)$
A	Nodes 1–10	0.046	10	Prefrontal cortex	6	3	0.044
				<b>Basal Ganglia</b>	<b>6</b>	<b>4</b>	<b><math>4.19 \times 10^{-3}</math></b>
				Septum/DB	4	1	0.502
	Nodes 33–64	0.033	32	Control hubs	19	0	1.000
				<b>Thalamus</b>	<b>11</b>	<b>11</b>	<b><math>1.74 \times 10^{-4}</math></b>
				Amygdala	3	3	0.119
				Basal ganglia	6	2	0.902
				Hippocampus	5	3	0.500
				Septum/DB	4	2	0.694
				Prefrontal cortex	6	1	0.989
				Medial prefrontal cortex	4	1	0.943
				Cortex	6	2	0.901
				<b>Control hubs</b>	<b>19</b>	<b>16</b>	<b><math>3.75 \times 10^{-4}</math></b>
	Nodes 54–64	0.026	11	<b>Thalamus</b>	<b>11</b>	<b>6</b>	<b><math>1.92 \times 10^{-3}</math></b>
				Hippocampus	5	1	0.624
Amygdala				3	1	0.438	
Basal ganglia				6	1	0.694	
<b>Control hubs</b>				<b>19</b>	<b>9</b>	<b><math>1.29 \times 10^{-4}</math></b>	
<b>Prefrontal cortex</b>				<b>6</b>	<b>6</b>	<b><math>6.16 \times 10^{-6}</math></b>	
B	Nodes 1–11	0.008	11	Cortex	6	2	0.273
				Thalamus	11	1	0.897
				PCP hubs	11	4	0.085
				<b>Medial prefrontal cortex</b>	<b>4</b>	<b>4</b>	<b><math>2.15 \times 10^{-3}</math></b>
	Nodes 29–43	0.007	15	Thalamus	11	4	0.229
				Septum/DB	4	3	0.037
				Mesolimbic	4	1	0.667
				Basal ganglia	6	2	0.432
				PCP hubs	11	1	0.961
				Basal ganglia	6	3	0.044
				<b>Hippocampus</b>	<b>5</b>	<b>5</b>	<b><math>3.31 \times 10^{-5}</math></b>
	Nodes 55–64	0.039	10	Amygdala	3	2	0.061
				PCP hubs	11	1	0.871

The hypergeometric probability of observing at least the number of brain regions from a given neural subsystem in clusters identified as being significantly different between control (reordering A) and PCP-treated (reordering B) animals. The significant presence of each cluster in the GSVD reordered matrix was confirmed by comparison with clustering in 1000 randomized permutations of the matrix (P-value, significance set at  $P < 0.05$ ). Criteria for the significant over abundance of a defined neural subsystem in a cluster were set at  $P(X \geq n) < 0.005$ . Subsystems found to be significantly over-represented within a given functional cluster are highlighted in bold.

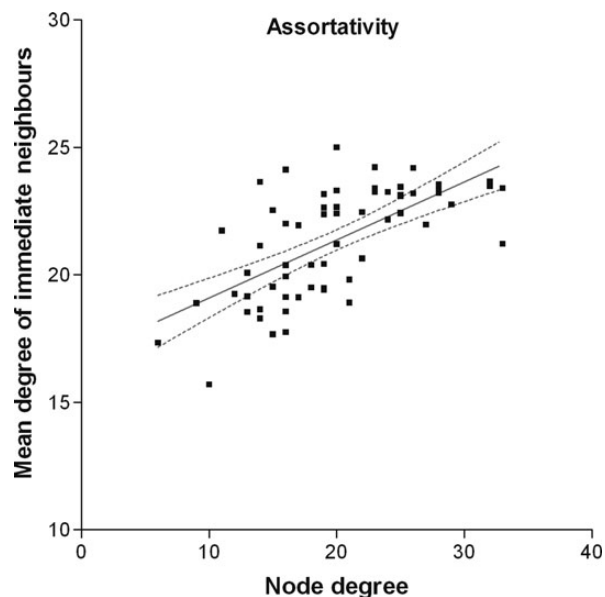


**Figure 4.** Assortativity in 2-DG functional brain networks. Brain regions in the functional brain network of control animals display the property of assortativity, which is the property that brain regions with high connectivity ( $k_i$ ) of connectivity are more likely to be connected to other brain regions with high connectivity. This is confirmed by a significant correlation (Pearson's  $r^2 = 0.429$ ,  $P < 0.001$ ) between regional degree ( $k_i$ ) and the mean degree of the regions to which that brain region is functionally connected.

that long-term potentiation of this direct HP–PFC projection is regulated by both LC neuronal activity and noradrenaline (NA; Lim et al. 2010). This suggests that the LC has a primary role in regulating the functional coupling between the PFC and HP through this direct projection. Therefore, it is of particular significance that we observed decreased connectivity of the LC in the functional brain network of PCP-treated animals. While the PFC receives direct innervation from the HP, there is no direct anatomical connection from the PFC to the HP (Vertes et al. 2007). Rather, the PFC influences neuronal activity in the HP through indirect pathways including the PFC–Re–HP pathway. Neurons from the PFC directly innervate neurons within the Re that in turn project to the CA1 and subiculum of the HP (Vertes 2002, 2004). The decreased functional connectivity (reduced centrality) of the Re in PCP-treated animals may impede on the ability of the PFC to modulate neuronal activity in the HP via this pathway, and vice versa. It is highly probable that alternative anatomical pathways through other thalamic nuclei, which are yet to be defined, are also disrupted and contributed to the compromised functional integration between these subsystems in PCP-treated animals. The specificity of subchronic NMDA receptor hypofunction in promoting hippocampal–PFC disintegration, and its potential contribution to the translationally relevant cognitive deficits seen in these animals (Egerton et al. 2005, 2008; Dawson et al. 2012), is further supported by our observation that acute modafinil treatment, which does

not induce similar cognitive deficits to those seen in PCP-treated animals (Waters et al. 2005) and has negligible affinity for NMDA receptors (Mignot et al. 1994), fails to induce the hippocampal–PFC functional disintegration seen in animals treated subchronically with PCP (Supplementary Material, Section 2).

Our results not only support compromised functional integration between distributed neural subsystems within the brain of PCP-treated animals, but also functional disintegration within defined brain subsystems in these animals. This effect is evident within both the thalamic and the basal ganglia subsystems, most notably, the functional dissociation of the substantia nigra [substantia nigra pars reticulata (SNR)] from the striatum (DLST, ventromedial striatum) in PCP-treated animals. These regions form a discrete functional cluster in control animals, which is lost in PCP-treated animals. Reciprocal anatomical projections exist between the striatum and substantia nigra (Haber et al. 2000) and form an essential component of brain circuitry involved in directing attention to important stimuli and in behavioral flexibility (Schultz et al. 2003). Functional disintegration between the striatum and substantia nigra in PCP-treated animals may contribute to the reduced behavioral flexibility seen in these animals (Egerton et al. 2005, 2008; Dawson et al. 2012). The functional disintegration of thalamic regions may result from the loss of the reticular thalamic nuclei (dRT/vRT) as important hubs in PCP-treated animals as these nuclei have reciprocal projections with and regulate the functional activity in all other thalamic nuclei (Crabtree and Isaac 2002). Furthermore, as the reticular thalamic nuclei intercept and modulate corticothalamic and thalamocortical projections, including projections between the PFC and thalamus (Zikopoulos and Barbas 2006), loss of these regions as hubs may contribute to the functional segregation of the PFC from other brain subsystems.

The alterations in regional centrality and clustering seen in PCP-treated animals also provide evidence for the dysfunction of specific neurotransmitter systems in these animals. In particular, reduced centrality of the LC suggests dysfunctional NA neurotransmission, whereas the functional disintegration of the substantia nigra and striatum supports dysfunctional dopamine neurotransmission in PCP-treated animals. Both of these neurotransmitter systems may play a role in the cognitive inflexibility previously reported in PCP-treated animals (Egerton et al. 2005, 2008; Dawson et al. 2012). NA neurotransmission not only regulates functional integration between the PFC and HP (Lim et al. 2010), but its levels in frontal cortical structures directly regulate behavioral flexibility (Tait et al. 2007; McGaughy et al. 2008). Furthermore, we have recently identified normalized functional coupling of the LC to cortical brain regions as an important mechanism contributing to the rescue of the behavioral inflexibility seen in PCP-treated animals by modafinil (Dawson et al. 2012). While dysfunction of noradrenergic neurotransmission in schizophrenia is widely supported (for review see Yamamoto and Hornykiewicz 2004), only recently have reports emerged supporting LC dysfunction in this disorder (Shibata et al. 2008), as has the suggestion that adrenergic neurotransmission represents a plausible target for the relief of the cognitive impairments in schizophrenia (Arnsten 2004; Harvey 2009). Dopamine dysfunction in the striatum of PCP-treated rats is supported by the functional disintegration of this region from the substantia nigra (SNR/SNC), which send

dopaminergic projections to the striatum (Andén et al. 1964). This mechanism may contribute to the striatal dopamine dysfunction reported in schizophrenia that also has a proposed role in the cognitive deficits seen in this disorder (Simpson et al. 2010).

In conclusion, our results provide strong evidence for NMDA receptor dysfunction as a unifying pathophysiological mechanism underlying the diverse mechanisms of brain dysfunction proposed to underlie the cognitive deficits seen in schizophrenia. These mechanisms include “compromised functional integration” between distributed brain subsystems (e.g. PFC–HP functional integration), the “functional disintegration” of discrete functional brain subsystems (e.g. the nigrostriatal pathway), thalamic disconnectivity as well as aberrant noradrenergic and dopaminergic neurotransmission in schizophrenia. We have shown, for the first time, that taking a systems approach to characterizing and quantifying altered brain function in a preclinical translational model provides greater insight into the mechanisms underlying brain dysfunction in psychiatric disease. Given the emerging evidence for brain network dysfunction in psychiatric disorders, taking a network science approach to characterizing brain dysfunction in translational models provides new opportunities for drug discovery for these disorders.

### Supplementary Material

Supplementary material can be found at: <http://www.cercor.oxfordjournals.org/>.

### Funding

This work was funded by the Psychiatric Research Institute of Neuroscience in Glasgow (PsyRING to N.D.), a joint initiative between the Universities of Glasgow and Strathclyde and the National Health Service of Greater Glasgow and Clyde; the Engineering and Physical Sciences Research Council Bridging the Gap Program (grant number EP/E018858/1 to N.D., J.A.P, D.J.H); the Engineering and Physical Sciences Research Council (grant number EP/E049370/1 to X.X., grant number EP/E049370/1 to D.J.H.), and the Medical Research Council (grant number G0601353 to D.J.H.). M.D is supported by an Engineering and Physical Sciences Research Council funded doctoral training grant in medical devices.

### Note

*Conflict of Interest:* None declared.

### References

- Andén NE, Carlsson A, Dahlström A, Fuxe K, Hillarp N, Larsson K. 1964. Demonstration and mapping out of nigro-neostriatal dopamine neurons. *Life Sci.* 3:523–530.
- Andreassen NC, O’Leary DS, Cizadlo T, Arndt S, Rezaei K, Boles Ponto LL, Leonard Watkins G, Hichwa RD. 1996. Schizophrenia and cognitive dysmetria: a positron emission tomography study of dysfunctional prefrontal-thalamic-cerebellar circuitry. *Proc Natl Acad Sci USA.* 93:9985–9990.
- Arnsten AFT. 2004. Adrenergic targets for the treatment of cognitive deficits in schizophrenia. *Psychopharmacology.* 174:25–31.
- Bassett DS, Bullmore E, Verchinski BA, Mattay VS, Weinberger DR, Meyer-Lindenberg AM. 2008. Hierarchical organization of human cortical networks in health and schizophrenia. *J Neurosci.* 28:9239–9248.

- Benetti S, Mechelli A, Picchioni M, Broome M, Williams S, McGuire P. 2009. Functional integration between the posterior hippocampus and prefrontal cortex is impaired in both first episode schizophrenia and the at risk mental state. *Brain*. 132:2426–2436.
- Bullmore ET, Frangou S, Murray RM. 1997. The dysplastic net hypothesis: an integration of developmental and dysconnectivity theories of schizophrenia. *Schizophr Res*. 28:143–156.
- Bullmore ET, Sporns O. 2009. Complex brain networks: graph theoretical analysis of structural and functional systems. *Nat Rev Neurosci*. 10:186–198.
- Cochran SM, Kennedy M, Mckerchar CE, Steward LJ, Pratt JA, Morris BJ. 2003. Induction of metabolic hypofunction and neurochemical deficits after chronic intermittent exposure to phencyclidine: differential modulation by antipsychotic drugs. *Neuropsychopharmacology*. 28:265–275.
- Cochran SM, McKerchar CE, Morris BJ, Pratt JA. 2002. Induction of differential patterns of local cerebral glucose metabolism and immediate-early genes by acute clozapine and haloperidol. *Neuropharmacology*. 43:394–407.
- Cosgrove J, Newell T. 1991. Recovery of neuropsychological function during reduction in use of phencyclidine. *J Clin Psychol*. 47:159–169.
- Crabtree JW, Isaac JTR. 2002. New intrathalamic pathways allowing modality-related and cross-modality switching in the dorsal thalamus. *J Neurosci*. 22:8754–8761.
- Danos P, Baumann B, Bernstein HG, Franz M, Stauch R, Northoff G, Krell D, Falkai P, Bogerts B. 1998. Schizophrenia and anteroventral thalamic nucleus: selective decrease of parvalbumin-immunoreactive thalamocortical projection neurons. *Psychiatry Res*. 82:1–10.
- Dawson N, Ferrington L, Lesch KP, Kelly PAT. 2011. Cerebral metabolic responses to 5-HT<sub>2A/C</sub> receptor activation in mice with genetically modified serotonin transporter (SERT) expression. *Eur Neuropsychopharmacol*. 21:117–128.
- Dawson N, Thompson RJ, McVie A, Thomson DM, Morris BJ, Pratt JA. 2012. Modafinil reverses phencyclidine (PCP)-induced deficits in cognitive flexibility, cerebral metabolism and functional brain connectivity. *Schizophr Bull*. 38:457–474.
- Egerton A, Reid L, McGregor S, Cochran SM, Morris BJ, Pratt JA. 2008. Subchronic and chronic PCP treatment produces temporally distinct deficits in attentional set shifting and prepulse inhibition in rats. *Psychopharmacology*. 198:37–49.
- Egerton A, Reid L, McKerchar CE, Morris BJ, Pratt JA. 2005. Impairment in perceptual attentional set-shifting following PCP administration: a rodent model of set-shifting deficits in schizophrenia. *Psychopharmacology*. 179:77–84.
- Ferino F, Thierry AM, Glowinski J. 1987. Anatomical and electrophysiological evidence for a direct projection from ammons horn to the medial prefrontal cortex in the rat. *Exp Brain Res*. 65:421–426.
- Ferraro L, Fuxe K, Tanganelli S, Fernandez M, Rambert FA, Antonelli T. 2000. Amplification of cortical serotonin release: a further neurochemical action of the vigilance-promoting drug modafinil. *Neuropharmacology*. 39:1974–1983.
- Friston KJ, Frith CD. 1995. Schizophrenia: a disconnection syndrome? *Clin Neurosci*. 3:89–97.
- Guillery RW, Sherman SM. 2002. Thalamic relay functions and their role in corticocortical communication: generalizations from the visual system. *Neuron*. 33:163–175.
- Haber SN, Fudge JL, McFarland NR. 2000. Striatonigrostriatal pathways in primates form an ascending spiral from the shell to the dorsolateral striatum. *J Neurosci*. 20:2369–2382.
- Harvey P. 2009. Pharmacological cognitive enhancement in schizophrenia. *Neuropsychol Rev*. 19:324–335.
- Hertzmann M, Reba RC, Kotlyarov EV. 1990. Single proton emission computer tomography in phencyclidine and related drug abuse. *Am J Psychiatry*. 147:255–256.
- Hilaire ZD, Orosco M, Rouch C, Blanc G, Nicolaidis S. 2001. Variations in extracellular monoamines in the prefrontal cortex and medial hypothalamus after modafinil administration: a microdialysis study in rats. *Neuroreport*. 12:3533–3537.
- Honey GD, Pomarol-Clotet E, Corlett PR, Honey RAE, McKenna PJ, Bullmore ET, Fletcher PC. 2005. Functional dysconnectivity in schizophrenia associated with attentional modulation of motor function. *Brain*. 128:2597–2611.
- Jay TM, Burette F, Laroche S. 1995. NMDA receptor-dependent long-term potentiation in the hippocampal afferent fiber system to the prefrontal cortex in the rat. *Eur J Neurol*. 7:247–250.
- Kim JJ, Kwon JS, Park HJ, Youn T, Kang DH, Kim MS, Lee DS, Lee MC. 2003. Functional disconnection between the prefrontal and parietal cortices during working memory processing in schizophrenia: a [<sup>15</sup>O]H<sub>2</sub>O PET study. *Am J Psychiatry*. 160:919–923.
- Kim JJ, Seok JH, Park HJ, Lee DS, Lee MC, Kwon LS. 2005. Functional disconnection of the semantic networks in schizophrenia. *Neuroreport*. 16:355–359.
- Laroche S, Davis S, Jay TM. 2000. Plasticity at hippocampal to prefrontal cortex synapses: dual roles in working memory and consolidation. *Hippocampus*. 10:438–446.
- Lim EP, Tan CH, Jay TM, Dawe GS. 2010. Locus coeruleus stimulation and noradrenergic modulation of hippocampal-prefrontal cortex long-term potentiation. *Int J Neuropsychopharmacol*. 4:1–13.
- Liu Y, Liang M, Zhou Y, He Y, Hao Y, Song M, Yu C, Liu H, Liu Z, Jiang T. 2008. Disrupted small-world networks in schizophrenia. *Brain*. 131:945–961.
- Lynall ME, Bassett DS, Kerwin R, McKenna PJ, Kitzbichler M, Muller U, Bullmore E. 2010. Functional connectivity and brain networks in schizophrenia. *J Neurosci*. 30:9477–9487.
- Madras BK, Xie ZH, Lin ZC, Jassen A, Panas H, Lynch L, Johnson R, Livni E, Spencer TJ, Bonab AA et al. 2006. Modafinil occupies dopamine and norepinephrine transporters in vivo and modulates the transporters and trace amine activity in vitro. *J Pharmacol Exp Ther*. 319:561–569.
- McGaughy J, Ross RS, Eichenbaum H. 2008. Noradrenergic, but not cholinergic, deafferentation of prefrontal cortex impairs attentional set-shifting. *Neuroscience*. 153:63–71.
- Meyer-Lindenberg AS, Olsen RK, Kohn P, Brown T, Egan MF, Weinberger DR, Berman KF. 2005. Regionally specific disturbance of dorsolateral prefrontal-hippocampal functional connectivity in schizophrenia. *Arch Gen Psychiatry*. 62:379–386.
- Micheloyannis S, Pachou E, Stam CJ, Breakspear M, Bitsios P, Vourkas M, Erimaki S, Zervakis M. 2006. Small-world networks and disturbed functional connectivity in schizophrenia. *Schizophr Res*. 87:60–66.
- Mignot E, Noshino S, Guilleminault C, Dement WC. 1994. Modafinil binds to the dopamine uptake carrier site with low affinity. *Sleep*. 17:436–437.
- Minzenberg MJ, Carter CS. 2008. Modafinil: a review of neurochemical actions and effects on cognition. *Neuropsychopharmacology*. 33:1477–1502.
- Olney JW, Labrugere J, Price MT. 1989. Pathological changes induced in cerebrocortical neurones by phencyclidine and related drugs. *Science*. 244:1360–1362.
- Paxinos G, Watson C. 1998. The rat brain in stereotaxic coordinates. London (UK): Academic Press Ltd.
- Peled A, Geva AB, Kremen WS, Blankfeld HM, Esfandiariard R, Nordahl TE. 2001. Functional connectivity and working memory in schizophrenia: an EEG study. *In J Neurosci*. 106:47–61.
- Pratt JA, Winchester CL, Dawson N, Morris BJ. 2012. Advancing schizophrenia drug discovery: optimizing rodent models to bridge the translational gap. *Nat Rev Drug Discov*. 11:560–579.
- Pratt JA, Winchester C, Egerton A, Cochran SM, Morris BJ. 2008. Modelling prefrontal cortex deficits in schizophrenia: implications for treatment. *Br J Pharmacol*. 153:S465–S470.
- Randall DC, Shneerson JM, Plaha KK, File SE. 2003. Modafinil affects mood, but not cognitive function, in healthy young volunteers. *Hum Psychopharmacol Clin Exp*. 18:163–173.
- Redrobe JP, Bull S, Plath N. 2010. Translational aspect of the novel object recognition task in rats abstinent following sub-chronic treatment with phencyclidine (PCP): effects of modafinil and relevance to cognitive deficits in schizophrenia. *Front Psychiatry*. 1:146.

- Schmahmann JD, Pandya DN. 2008. Disconnection syndromes of basal ganglia, thalamus, and cerebrocerebellar systems. *Cortex*. 44:1037–1066.
- Schultz W, Tremblay L, Hollerman JR. 2003. Changes in behavior-related neuronal activity in the striatum during learning. *Trends Neurosci*. 26:321–328.
- Shibata E, Sasaki M, Tohyama K, Otsuka K, Endoh J, Terayama Y, Sakai A. 2008. Use of neuromelanin sensitive MRI to distinguish schizophrenic and depressive patients and healthy individuals based on signal alterations in the substantia nigra and locus coeruleus. *Biol Psychiatry*. 64:401–406.
- Simpson EH, Kellendonk C, Kandel E. 2010. A possible role for the striatum in the pathogenesis of the cognitive symptoms of schizophrenia. *Neuron*. 65:585–596.
- Sokoloff L, Reivich M, Kennedy C, Des Rosiers MH, Patlak CS, Petti-grew KD, Sakurada O, Shinohara M. 1977. <sup>14</sup>C-Deoxyglucose method for measurement of local cerebral glucose-utilization— theory, procedure, and normal values in conscious and anesthe-tized albino-rat. *J Neurochem*. 28:897–916.
- Steward LJ, Kennedy MD, Morris BJ, Pratt JA. 2004. The atypical anti-psychotic drug clozapine enhances chronic PCP-induced regu-lation of prefrontal cortex 5-HT<sub>2A</sub> receptors. *Neuropharmacology*. 47:527–537.
- Tait DS, Brown VJ, Farovik A, Theobald DE, Dalley JW, Robbins TW. 2007. Lesions of the dorsal noradrenergic bundle impair attentional set-shifting in the rat. *Eur J Neurosci*. 25: 3719–3724.
- Turner DC, Clark L, Pomarol-Clotet E, McKenna P, Robbins TW, Saha-kian BJ. 2004. Modafinil improves cognition and attentional set shifting in patients with chronic schizophrenia. *Neuropsychophar-macology* 29:1363–1373.
- Vertes RP. 2002. Analysis of projections from the medial prefrontal cortex to the thalamus in the rat, with emphasis on nucleus re-uniens. *J Comp Neurol*. 442:163–187.
- Vertes RP. 2004. Differential projections of the infralimbic and prelim-bic cortex in the rat. *Synapse*. 51:32–58.
- Vertes RP, Hoover WB, Szgeti-Buck K, Leranath C. 2007. Nucleus re-uniens of the midline thalamus: link between the medial prefrontal cortex and the hippocampus. *Brain Res Bull*. 71:601–609.
- Waters KA, Burnham KE, O'Connor D, Dawson GR, Dias R. 2005. As-sessment of modafinil on attentional processes in a five-choice serial reaction time test in the rat. *J Psychopharmacology*. 19:149–158.
- Weinberger DR, Berman KF, Suddath R, Torrey EF. 1992. Evidence of dysfunction of a prefrontal-limbic network in schizophrenia: a mag-netic resonance imaging and regional cerebral blood flow study of discordant monozygotic twins. *Am J Psychiatry*. 149:890–897.
- Welsh RC, Chen A, Taylor SF. 2010. Low-frequency BOLD fluctuations demonstrate altered thalamocortical connectivity in schizophrenia. *Schizophr Bull*. 36:713–722.
- Wu JC, Buchsbaum MS, Patkin SG, Wolf MJ, Bunney WE. 1991. Posi-tron emission tomography study of phencyclidine users. *Schi-zophr Res*. 4:415.
- Xiao X, Dawson N, MacIntyre L, Morris BJ, Pratt JA, Watson DG, Higham DJ. 2011. Exploring metabolic pathway disruption in the subchronic phencyclidine model of schizophrenia with the gener-alized singular value decomposition. *BMC Syst Biol*. 5:72.
- Yamamoto K, Hornykiewicz O. 2004. Proposal for a noradrenaline hypothesis of schizophrenia. *Prog Neuropsychopharmacol Biol Psychiatry*. 28:913–922.
- Zikopoulos B, Barbas H. 2006. Prefrontal projections to the thalamic reticular nucleus form a unique circuit for attentional mechanisms. *J Neurosci*. 26:7348–7361.